

Contract No. NAS8-11083

INVESTIGATION OF BREMSSTRAHLUNG
PRODUCTION IN A SHIELDING MATERIAL

FACILITY FORM 802

N 66-12185	
(ACCESSION NUMBER)	(THRU)
16	1
(PAGES)	(CODE)
CR 68107	29
(NASA CR OR TMX OR AD NUMBER)	(CATEGORY)

Report Prepared For:

GEORGE C. MARSHALL SPACE FLIGHT CENTER
National Aeronautics & Space Administration
Huntsville, Alabama

May, 1965

ADVANCED RESEARCH CORPORATION
715 Miami Circle, N. E.
Atlanta, Georgia

GPO PRICE \$ _____

CFSTI PRICE(S) \$ _____

Hard copy (HC) 1.00

Microfiche (MF) .50

C O N T E N T S

	PAGE
Investigation of Bremsstrahlung production in a shielding material.	1
1. Introduction	1
2. The infinite slab shielding problem.	1
3. Numerical calculations	3
Results	10

LIST OF FIGURES

- Fig. 1. Electron Source Spectrum
2. Stopping Power of Aluminum for Electrons
3. Range of Electrons in Aluminum
4. Gamma Attenuation Function
5. Contributions to the Dose Rate in Roentgen per
 Hour from Various Regions of the E_0 - k plane.

LIST OF TABLES

Table	I	Mesh points and weight factors for integration over Θ .
	II	E_0 and x values used in evaluation of $\bar{\Phi}(E_0, x)$.
	III	k values used in the evaluation of $W(k, x)$.

INVESTIGATION OF BREMSSTRAHLUNG PRODUCTION IN A SHIELDING MATERIAL

1. Introduction

The situation to be considered is that of a space vehicle in an electron field. Because of the exploratory nature of this investigation an infinite slab embedded in an isotropic electron source is considered. In the following the general problem is considered along with various alternative simplifying assumptions. A model is then arrived at which can be handled simply with routine numerical methods. A description of a numerical calculation based on this simplified model will then be given. This calculation has a twofold objective: (1) to determine the electron-photon energy regions from which the major contributions to a dose rate come, the purpose here being to ascertain how well the Bremsstrahlung production cross-section must be known; and, (2) to evaluate the dose rate from the shielding, this latter result being only of secondary importance. A proposal for a convenient procedure of evaluating the dose rate due to arbitrary electron source spectra will also be given.

2. The Infinite Slab Shielding Problem

The problem is conveniently divided into five parts: the electron source spectrum, the electron penetration, the Bremsstrahlung production, the photon penetration, and the photon flux-to-dose conversion. Let $\Phi_S(E)dE$ be the flux of electrons in space with energies in dE about E ; and, let $G(E, E_0, x, \Theta)$ be the electron attenuation function so that the flux of electrons at a depth x with energies in dE_0 about E_0 whose momenta lie in the solid angle $d\Omega = \sin \Theta d\Theta d\phi$ and which result from electrons of energy E in the source spectrum is given by $\frac{1}{2} \Phi_S(E) G(E, E_0, x, \Theta) dE dE_0 d\Omega$. The factor of $1/2$ results from the hemispherical isotropy of the source when the slab is present. The angle Θ is measured with respect to the slab normal in the direction of penetration.

Now let $\frac{d^2\sigma}{dkd\Omega_0}(E_0, k, \Theta_0)$ be the cross-section for the production of Bremsstrahlung with energies in dk at k and momenta in the solid angle $d\Omega_0 = \sin \Theta_0 d\Theta_0 d\phi_0$ by electrons of energy E_0 where Θ_0 is the angle between the electron and the photon momenta and ϕ_0 is the corresponding azimuth.

The resulting photon flux produced in a thickness dx at x of the slab and differential in the indicated quantities is given by:

$$\frac{1}{2} N \Phi_s(E) G(E, E_0, x, \Theta) \frac{d^2\sigma}{dkd\Omega_0}(E_0, k, \Theta_0) dk dE dE_0 d\Omega d\Omega_0$$

where N is the number of atoms per unit volume of the shield. In arriving at this expression it was assumed that the slab consisted of a single element. If this is not the case one must sum $N\sigma$ over the different elements.

In order to introduce the gamma attenuation function it is convenient, at least formally, to make a change in the photon angle variables. For fixed (Θ, ϕ) make the transformation $(\Theta_0, \phi_0) \rightarrow (\xi, \zeta)$ where (ξ, ζ) are the spherical coordinate angles of the photon momentum as measured from the same axes as (Θ, ϕ) . Since Θ_0 is the angle between the electron and photon momenta it follows that

$$\cos \Theta_0 = \sin \Theta \sin \xi \cos (\phi - \zeta) + \cos \Theta \cos \xi$$

Using the new variables one can introduce the gamma attenuation function including build-up, $H(k, a-x, \xi)$, for photons of energy k produced at a depth x in a slab of thickness a and having momenta in the solid angle $d\Omega' = \sin \xi d\xi d\zeta$. Multiplying the photon flux obtained above by $k\lambda(k)$ times this function and integrating over all variables gives the Bremsstrahlung dose rate after penetration of the slab. $\lambda(k)$ is the energy flux to dose ratio. Of course, the functions G , H and σ are not well known over the entire range of variables. In fact, only for $\frac{d\sigma}{dk}$ are there closed form expressions available and these are at best approximations. Thus even to make numerical evaluations of the dose rate one must adopt a

simplified model for the electron and photon penetrations.

Three simplifying assumptions considered are:

- (1) Straight-ahead, continuous slowing down of the penetrating electrons.

This requires that G have the form

$$G(E, E_0, x, \Theta) = \frac{S(E)}{2\pi S(E_0)} \delta \left[E - R^{-1}(R(E_0) + x/\cos\Theta) \right] \quad \text{for } 0 \leq \Theta \leq \pi/2$$

$$= 0 \quad \text{for } \pi/2 \leq \Theta \leq \pi$$

where $S(E)$ = stopping power for electrons of energy E

$R(E_0)$ = range of electrons of energy E_0

$R^{-1}(\eta)$ = energy of electrons with range η

and δ denotes the Dirac δ -function.

$x/\cos \Theta$ is simply the crow-flight distance traveled by the electron in reaching the depth x , and $R(E_0)$ is the electron's residual range after reaching this depth. The sum of these two members must be the total range of the electron which must correspond to the electron's initial energy E . This is the reason for the δ -function in G .

(2) Straight-ahead Bremsstrahlung production. This means that the Bremsstrahlung production cross-section is integrated over the solid angle $d\Omega_0$ and the photon is assigned the momentum direction of the ingoing electron. In this situation the transformation $(\Theta_0, \phi_0) \rightarrow (\xi, \zeta)$ is unnecessary and $H(k, a-x, \xi)$ becomes $H(k, a-x, \Theta)$. If buildup is neglected one can give the explicit expression $H(k, a-x, \Theta) = e^{-\frac{\mu(a-x)}{\cos \Theta}}$ where μ is the appropriate attenuation coefficient for photons of energy k .

(3) Plane source of isotropic radiation at each depth x . This again means that the Bremsstrahlung production cross-section is integrated over $d\Omega_0$. In this case, however, $H(k, a-x, \xi)$ is replaced by $A(a-x, k) = E_1(\mu(a-x)) = \int_0^\infty e^{-t} \frac{dt}{t} \frac{1}{\mu(a-x)}$. The transformation $(\Theta_0, \phi_0) \rightarrow (\xi, \zeta)$ is again unnecessary.

In the numerical calculation to be described shortly the assumptions (1) and (3) were used. A slight modification, however, would accommodate (2) instead of (3). Under the assumptions (1) and (3) the dose rate D is given by

$$D = \int_0^{\infty} dE_0 \int_0^{E_0-1} dk \int_0^a dx \int_0^{\pi/2} \sin \Theta d\Theta f(E_0, k, x, \Theta)$$

where

$$f(E_0, k, x, \Theta) = 1/2 Nk \lambda(k) \Phi_s(E) \frac{S(E)}{S(E_0)} \frac{d\sigma(E_0, k)}{dk} A(a-x, k)$$

with E evaluated at $R^{-1}[R(E_0) + x/\cos\Theta]$. The units have been chosen so that

$m = h = c = 1$ where m is the electron mass. The order of integration has been chosen so that the contributions to D from various E_0, k regions can be easily investigated. Since this was the prime purpose of the numerical calculation this expression is the appropriate one. An alternate expression, convenient for investigating the dependence on the source spectrum, is given for completeness:

$$D = \int_0^{\infty} dE \int_0^{E-1} dE_0 \int_0^{E_0-1} dk \int_0^a dx f^1(E, E_0, k, x)$$

with f^1 identical in form to f. This order of integration is somewhat difficult to handle on a desk calculator due to the large number of mesh points at which $\frac{d\sigma}{dk}(E_0, k)$ must be known. However, once the first three integrals have been evaluated, with, perhaps, the aid of a digital computer code for $\frac{d\sigma}{dk}$, the remaining quadrature over E can be handled in a routine fashion on a desk calculator.

3. Numerical Calculations

A rather crude preliminary calculation was made for an aluminum slab having a thickness of 4 gm/cm². In this preliminary calculation a five-point Gaussian quadrature over Θ was first performed followed by a nine-point trapezoidal integration over x. The $E_0 - k$ plane was then divided into rectangles with six divisions along the E_0 axis and fourteen divisions along the k axis. The contribution to the dose rate from

each rectangle was then obtained by multiplying the area of each rectangle by the mean value of the integrand of D at the four corners.

Clearly the number of mesh points used was not sufficient to warrant conclusions about relative contributions from various parts of the E_0 - k plane. However, the calculation was fruitful in helping the investigators make a more judicious choice of mesh points for a second calculation.

In the second calculation a nine-point Gaussian integration was used to evaluate the integral over Θ :

$$\Phi(E_0, X) = \frac{1}{2} \int_0^{\pi/2} \Phi_s(E) \frac{S(E)}{S(E_0)} \sin \Theta d\Theta = \frac{1}{2} \int_0^1 \Phi_s(E) \frac{S(E)}{S(E_0)} d(\cos \Theta)$$

This expression gives the electron flux per unit energy at energy E_0 and depth x . The mesh points, $\cos \Theta_i$, $i=1, \dots, 9$, and weight factors, w_i , used for this quadrature are listed in table I. The source spectrum used in this calculation was an enlarged smooth curve drawn from information obtained from Messrs. H. E. Stern and M. O. Burrell, MSFC, Huntsville, who in turn obtained it as a private communication from Hess and his coworkers at Goddard SFC. See figure 1. It represents the integral over typical orbits in the artificial trapped belt over a period of two days. Enough orbits were considered so that the effects of any anisotropies were averaged out; thus the electron flux may be considered as being isotropic. The range and stopping power data were obtained from the published results of Berger and Seltzer³⁾. See figures 2 and 3. The total stopping power was used which includes contributions from collision and radiation.

TABLE I

Mesh points and weight factors for integration over Θ^2 .

i	Θ_i (approx.)	$\cos \Theta_i$	w_i
1	89.1°	.015920	.04064
2	85.3°	.08198	.09032
3	78.9°	.19331	.13031
4	70.3°	.3379	.15617
5	60°	.5000	.16512
6	48.5°	.6621	.15617
7	36.2°	.8067	.13031
8	23.3°	.9180	.09032
9	10.2°	.9841	.04064

The E_0 and x values used in the evaluation of $\bar{\Phi}$ are listed in Table II.

Also listed in Table II are the weight factors W_x used in the subsequent integration over x .

TABLE II

E_0 and x values used in evaluation of $\bar{\Phi}$ (E_0, x)

E_0 (mc ²)	x (gm/cm ²)	W_x
1.25	0	.0625
1.50	.125	.1250
2	.25	.1250
3	.375	.1250
4	.50	.1875
5	.75	.3750
6	1.25	.5000
7.5	1.75	.5000
10	2.25	.5000
11	2.75	.5000
12	3.25	.5000
	3.75	.3750

After the evaluation of Φ the quantity

$$W(k, x) = \lambda(k) A(a-x, k)$$

was evaluated for the x values in table II and for the k values in table III. It was convenient here to use new units for the photon energies, k , since the data for $\mu^{4)}$ and $\lambda^{5)}$ were given in these units. A factor of .511 was included in W to account for this change of units. Figure 4 shows $E_1(Z)$ vs. Z used in the evaluation of $A^{6)}$.

TABLE III

k values used in the evaluation of $W(k, x)$

k (mev)
.01
.05
.1
.3
.5
.7
1.0
1.5
2.0
3.0
5.0
10.0

The integral

$$I(E_0, K) = \int_0^4 \Phi(E_0, x) W(k, x) dx$$

was then evaluated using the trapezoidal rule for unequal intervals. The weight factors for this integration are tabulated in Table II. In terms of I the dose rate is given by

$$D = N \int_0^\infty dE_0 \int_0^{E_0-1} k \frac{d\sigma}{dk}(E_0, k) I(E_0, k)$$

To evaluate this the E_0 - k plane was divided into a number of rectangles, triangles, and similar areas as indicated in figure 5. The contribution to D from each such area was approximated by the mean value of $Nk \frac{d\sigma}{dk} I$ at the corners multiplied by the area. Two expressions were used for $k \frac{d\sigma}{dk}$: one was formula 3 B N of reference 6; and, the other was 3 B N corrected at the high k end by the Elwert factor⁷⁾ and at the low k end by smoothing 3 B N into the value obtained from formula 10.1 of reference 8 with zero slope. The corresponding results for D will be denoted by D_{3BN} and D_{cor} , respectively. The contributions to D_{3BN} were only considered for those regions where $RR_0 < 1.20$ and $1/2 (\alpha_1 + \alpha_2) > .80$ ⁹⁾.

The values for 3BN were obtained by evaluating the cross-section at a sufficient number of k values to obtain a smooth curve for $E_0 = 1.25, 1.5, 3, 6, 10, 12 \text{ mc}^2$ ¹⁰⁾. Cross plots were then made in order to obtain the cross-sections at all necessary points. Cross plots of I were also made where necessary.

RESULTS

The results of the calculations are also indicated in the figure 5, with the contributions to the dose rate in roentgens per hour given in each area. The number preceded by the letter c is the value obtained using the corrected cross-section while the other value was obtained using 3 B N. The regions where either $1/2 (\alpha_1 + \alpha_2) < 0.80$ or $RR_O > 1.20$ are shaded.

The total dose rate for D_{cor} was 8183 R/hr. of which 7178 R/hr (94.4%) came from the region where $RR_O < 1.20$ and $1/2(\alpha_1 + \alpha_2) > 0.80$, 119 R/hr. (1.45%) from the region where $RR_O > 1.20$ and 346 R/hr. (4.22%) from the region where $1/2 (\alpha_1 + \alpha_2) < 0.80$.

Within the region where $RR_O < 1.20$ and $1/2 (\alpha_1 + \alpha_2) > .80$, $D_{3BN} = 7438$ R/hr. which is 3.29% less than the corresponding contribution to D_{cor} .

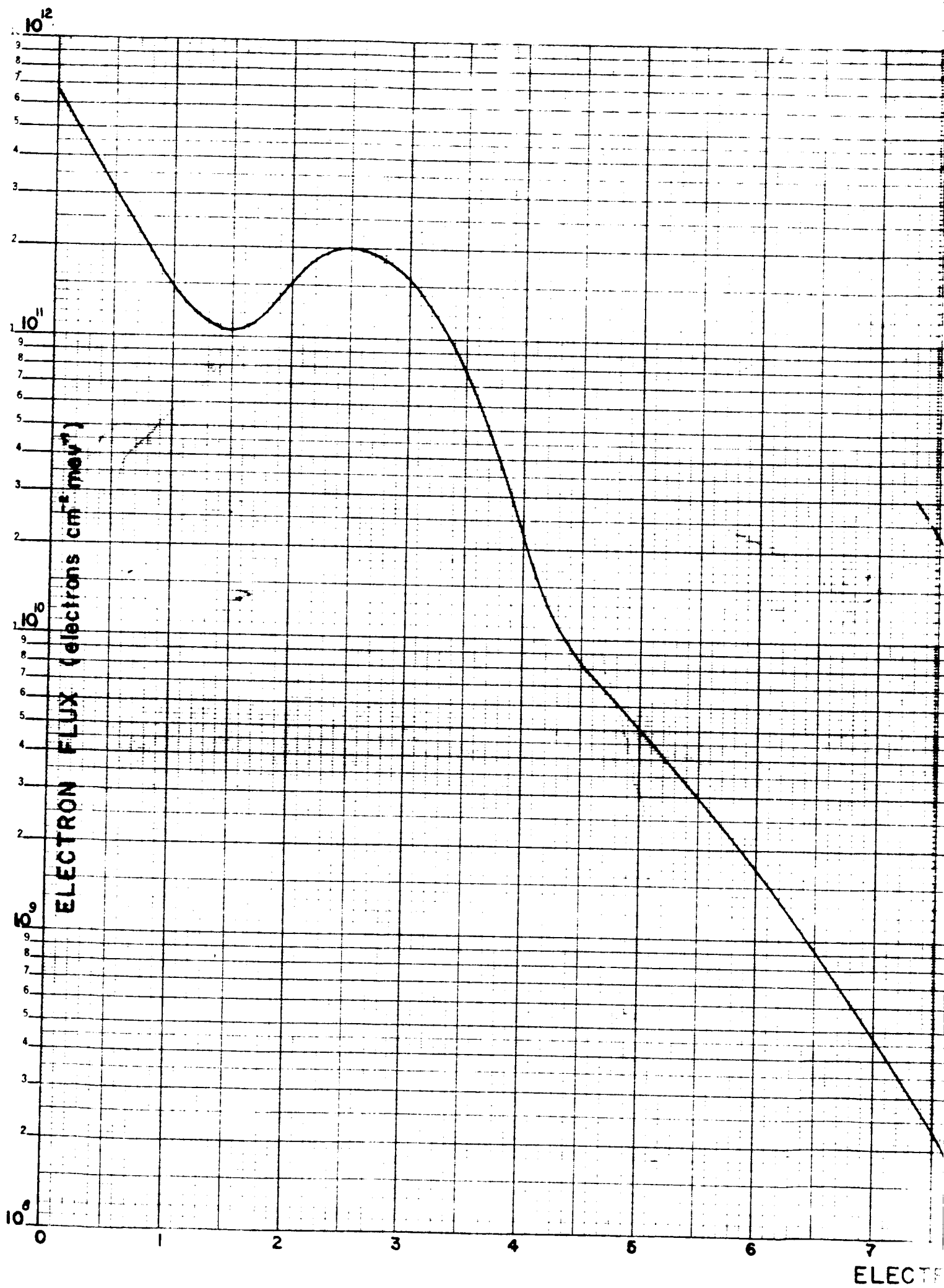
The smooth curves used for $k \frac{d\sigma}{dk}$ in the corrected case did not fall 20% lower than 3 B N at those places where $1/2 (\alpha_1 + \alpha_2) = 0.80$ as would be expected. A more careful plotting of these curves would undoubtedly lower the contribution to D_{cor} in the region where $RR_O < 1.20$ and $1/2 (\alpha_1 + \alpha_2) > 0.80$ by about 1.5%. This would bring it more in line with the value for D_{3BN} which is nice. However, it is doubtful that this is significant since the compensations in 3 B N which seem to bring it into line with the corresponding D_{cor} result from opposite ends of the curve $k \frac{d\sigma}{dk}$ vs. k .

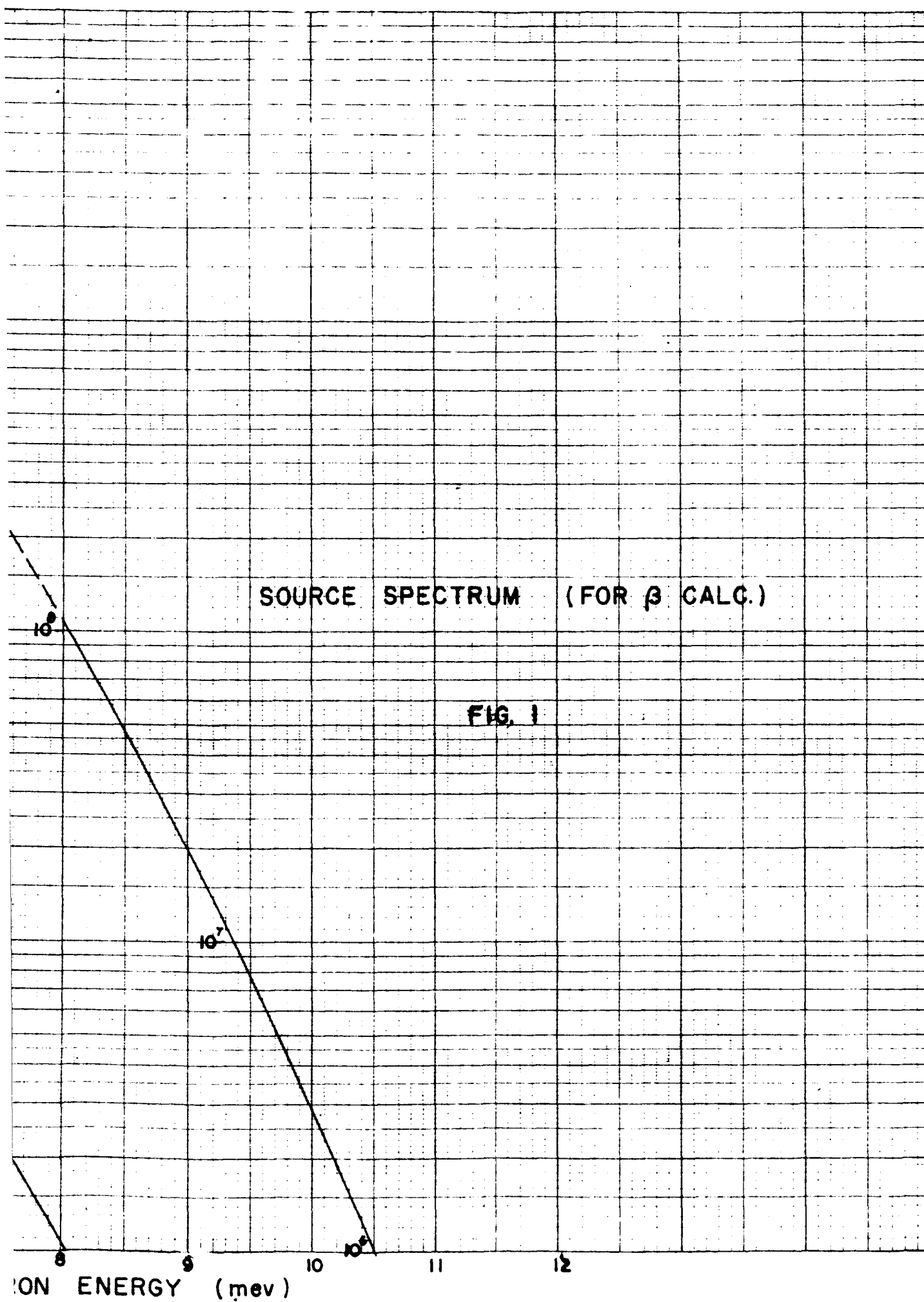
It should be noted that the relative importance of the contributions from various parts of the Bremsstrahlung production cross-section $\frac{d\sigma}{dk}(E_O, k)$ can be determined from figure 5 simply by summing the contributions from the regions of interest and comparing with the total dose rate. One should keep in mind here that E_O is the energy of the electron just prior to photon emission and not the energy of the electron before entering the slab.

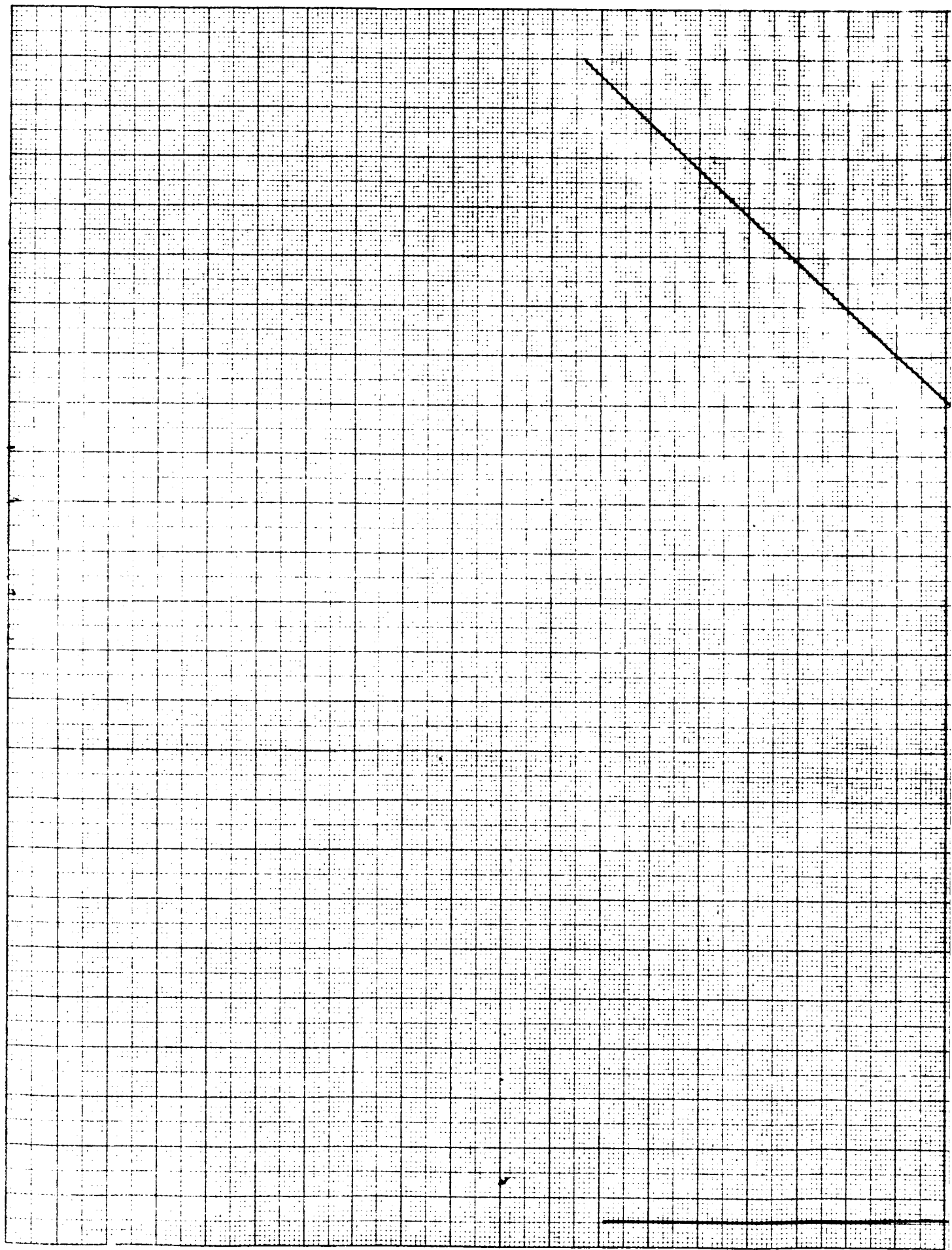
REFERENCES

- 1). In the calculations the slab thickness was measured in gm/cm^2 . In these units $N = 2.235 \times 10^{22}$ atoms/gm.
- 2). Obtained from equation 25.4.30 and table 25.4 of the Handbook of Mathematical Functions, AMS55, National Bureau of Standards.
- 3). M. J. Berger and S. M. Seltzer, Tables of Energy Losses and Ranges of Electrons and Positrons, NASA SP-3012.
- 4). Gamma-ray mass attenuation coefficients were obtained from Table 7 - 9 of Reactor Physics Constants, ANL-5800.
- 5). Gamma energy flux to dose conversion factors were obtained from NBS circular 583, X-ray Attenuation Coefficients from 10 Kev to 100 mev, by G. W. Grodstein; Supplement to NBS Circular 583, by R. J. McGinnies; p. 470 of ANL 5800, Reactor Physics Constants; and, 1960 Annual Report, Shielding Problems in Manned Space Vehicles, Lockheed-Georgia Company.
- 6). Data obtained from table 28a, p. 155, of Introduction to the theory of Neutron Diffusion, Volume 1, AEC.
- 7). H. W. Koch and J. W. Motz, Bremsstrahlung Cross-Section Formulas and Related Data, Rev. Mod. Phys., 31, 920 (1959).
- 8). See section E of reference 7.
- 9). R. L. Gluckstern and M. H. Hull, Jr., Polarization Dependence of the Integrated Bremsstrahlung Cross Section, Phys. Rev. 90, 1030 (1953).
- 10). See pages 10 and 13 of Bremsstrahlung Production Cross Sections for Shielding Against Electrons in Space, Advanced Research Corp., May, 1965.
- 11). See figures 2.31 of reference 10.

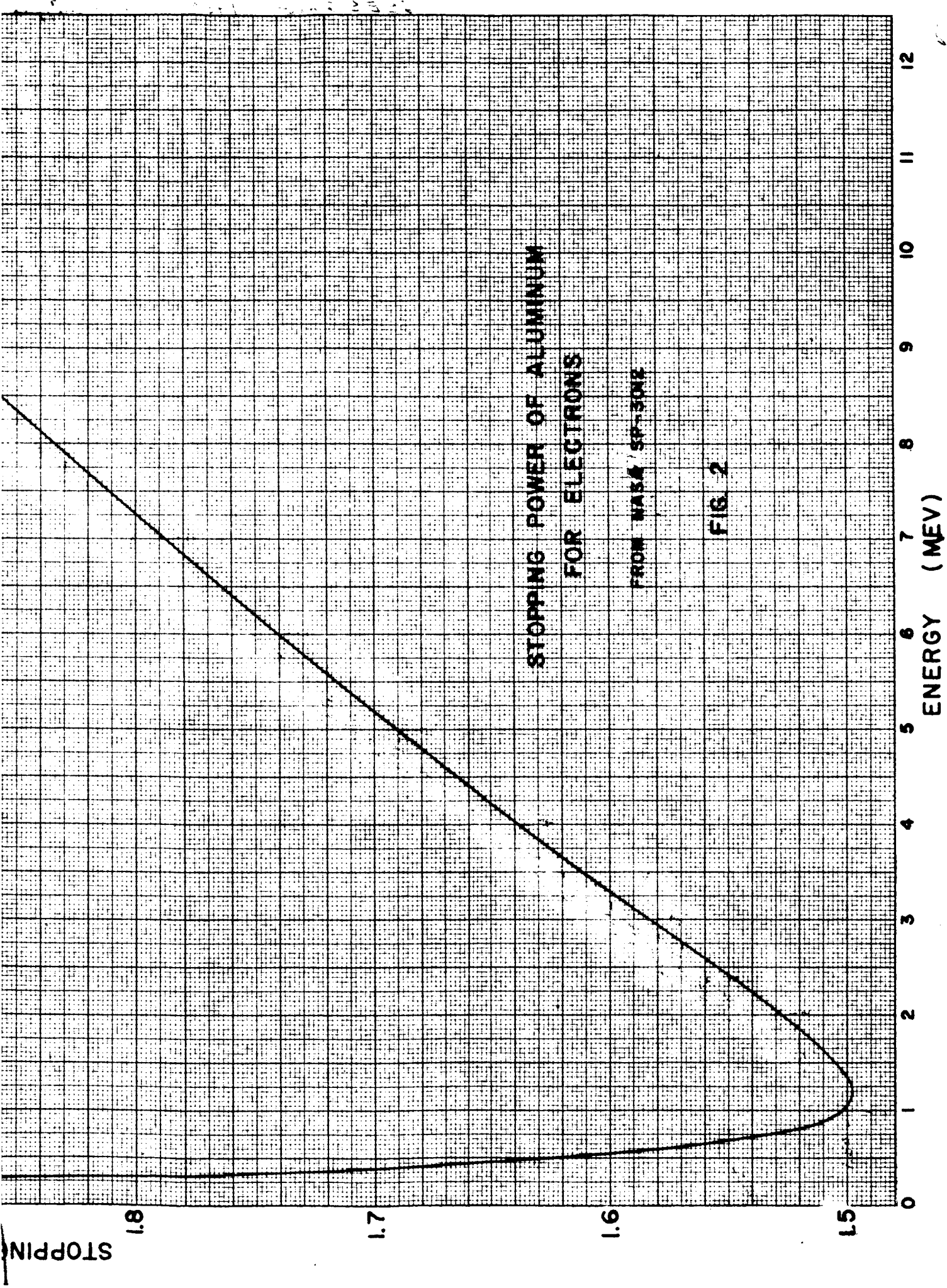
K&E SEMI LOGARITHMIC 358-81L
 KEUFFEL & ESSER CO. MADE IN U.S.A.
 4 CYCLES X 150 DIV 5.046



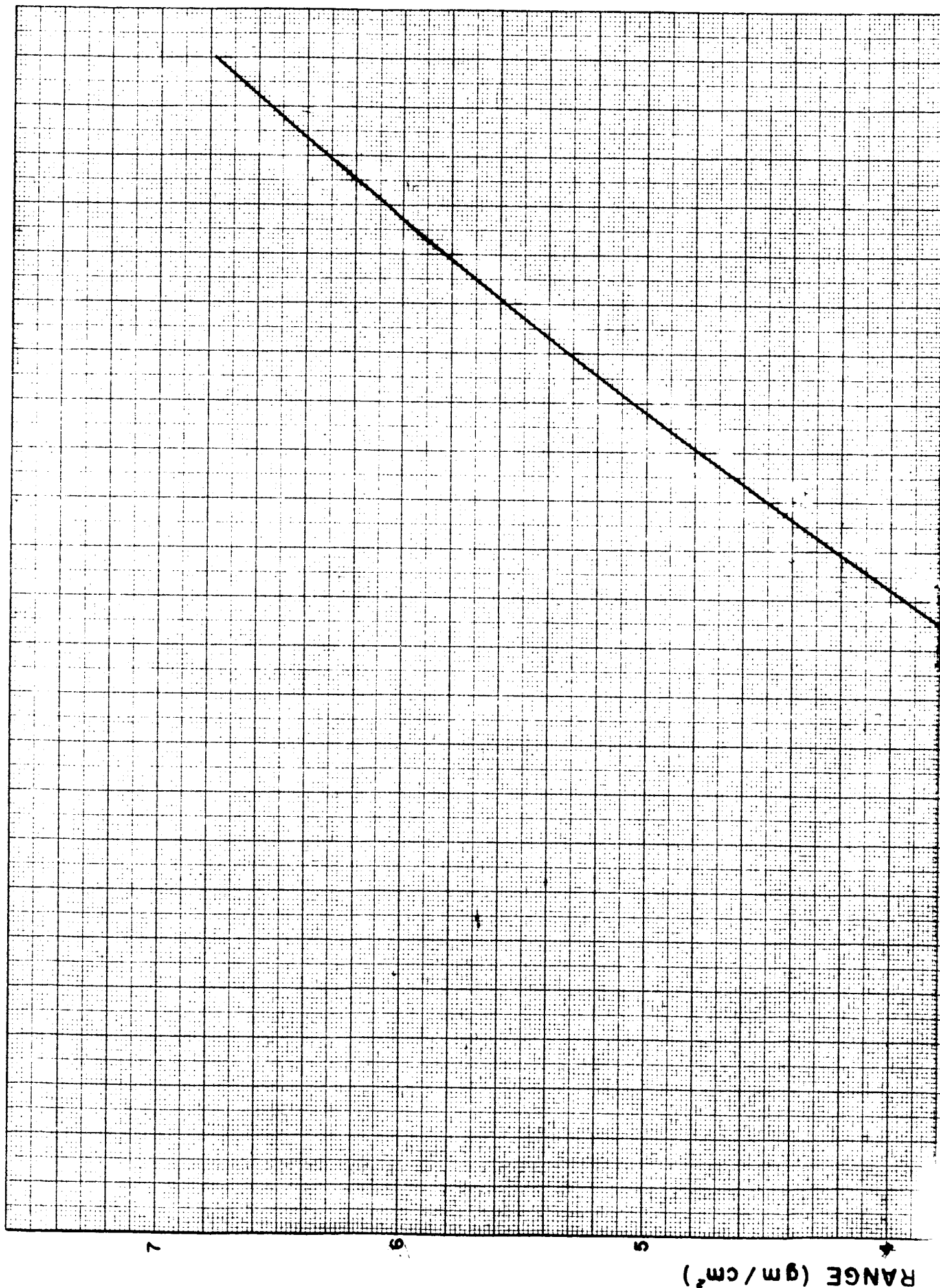


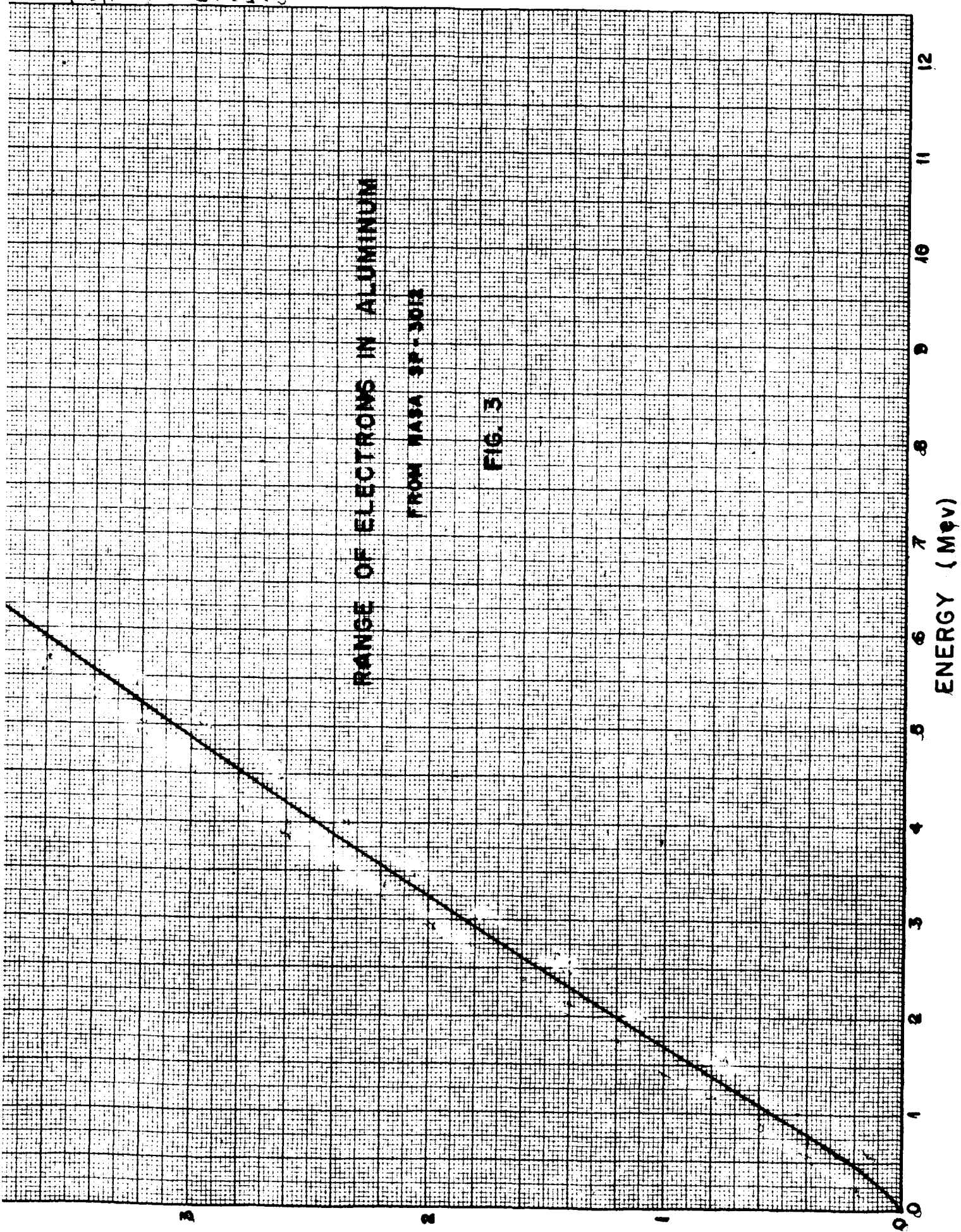


POWER (mev cm²/gm)
2.0



K&E 10 X 10 TO THE CENTIMETER 47 1516
25 X 25 CM • ALBANY, N.Y.
KEUFFEL & ESSER CO





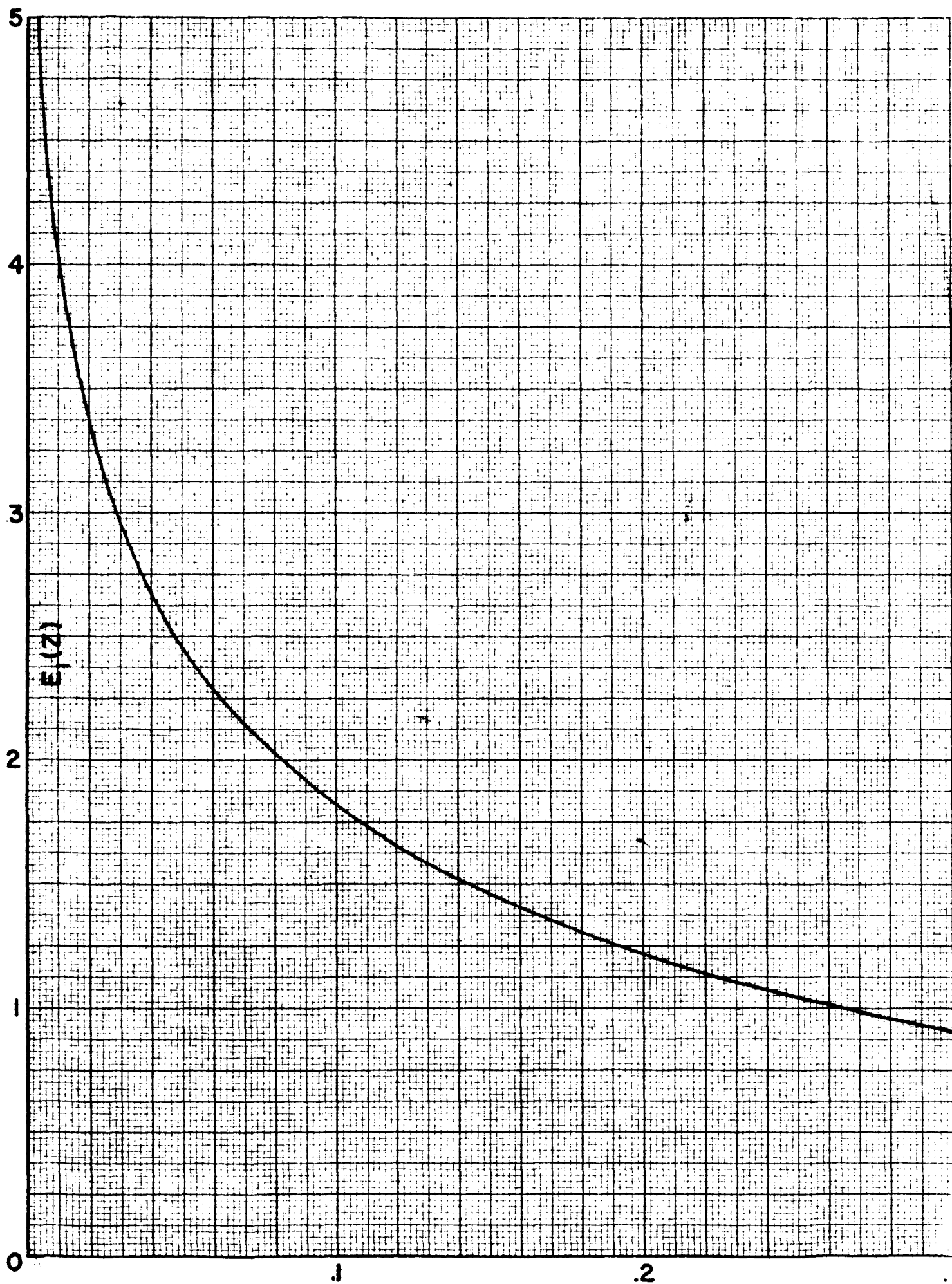
RANGE OF ELECTRONS IN ALUMINUM

FROM NASA SP-3012

FIG. 3

0-2-5-10-15-20-25-30-35-40-45-50-55-60-65-70-75-80-85-90-95-100

K-E 10 X 10 TO THE 1/2 INCH 359-11L
KEUPPEL & ESSER CO. MADE IN U.S.A.



GAMMA ATTENUATION FUNCTION

FIG. 4

